

# InP/ZnS Quantum Dots Cause Inflammatory Response in Macrophages Through Endoplasmic Reticulum Stress and Oxidative stress

This article was published in the following Dove Press journal:  
*International Journal of Nanomedicine*

Shuzhen Chen <sup>1</sup>  
Yajing Chen <sup>2</sup>  
Yenhua Chen<sup>1</sup>  
Zhengyuan Yao<sup>1</sup>

<sup>1</sup>Key Laboratory of Functional and Clinical Translational Medicine, Department of Basic Medicine, Xiamen Medical College, Xiamen 361023, People's Republic of China; <sup>2</sup>Department of Clinical Medicine, Xiamen Medical College, Xiamen 361023, People's Republic of China

**Purpose:** Quantum dots (QDs) are widely used semiconductor nanomaterials. Indium phosphide/zinc sulfide (InP/ZnS) QDs are becoming potential alternatives to toxic heavy metal-containing QDs. However, the potential toxicity and, in particular, the immunotoxicity of InP/ZnS QDs are unknown. This study aimed to investigate the impacts of InP/ZnS QDs on inflammatory responses both in vivo and in vitro.

**Methods:** Mice and mouse bone marrow-derived macrophages (BMMs) were exposed to polyethylene glycol (PEG) coated InP/ZnS QDs. The infiltration of neutrophils and the release of interleukin-6 (IL-6) were measured using a hematology analyzer and an enzyme-linked immunosorbent assay (ELISA) for the in vivo test. Cytotoxicity, IL-6 secretion, oxidative stress and endoplasmic reticulum (ER) stress were studied in the BMMs, and then, inhibitors of oxidative stress and ER stress were used to explore the mechanism of the InP/ZnS QDs.

**Results:** We found that 20 mg/kg PEG-InP/ZnS QDs increased the number of neutrophils and the levels of IL-6 in both peritoneal lavage fluids and blood, which indicated acute phase inflammation in the mice. PEG-InP/ZnS QDs also activated the BMMs and increased the production of IL-6. In addition, PEG-InP/ZnS QDs triggered oxidative stress and the ER stress-related PERK-ATF4 pathway in the BMMs. Moreover, the inflammatory response caused by the PEG-InP/ZnS QDs could be attenuated in the macrophages by blocking the oxidative stress or the ER stress with inhibitors.

**Conclusion:** InP/ZnS QDs can activate macrophages and induce acute phase inflammation both in vivo and in vitro, which may be regulated by oxidative stress and ER stress. Our present work is expected to help clarify the biosafety of InP/ZnS QDs and promote their safe application in biomedical and engineering fields.

**Keywords:** quantum dots, indium phosphide, inflammation, endoplasmic reticulum stress, reactive oxygen species

## Introduction

Quantum dots (QDs) are widely used semiconductor nanomaterials because they have excellent optical properties, including high quantum yield, size-controlled fluorescence, narrow emission spectra, strong emission, and low sensitivity to photo-bleaching. QDs are extensively applied in lighting, solar energy, optical sensing, and biomedical labeling and imaging.<sup>1-3</sup> Thus far, mainly group II-VI or IV-VI QDs have been applied, including, for example, CdTe, CdSe, and CdS.<sup>4,5</sup> Since they have toxic heavy metal elements (Cd or Pb), the potential health and environmental risks

Correspondence: Shuzhen Chen  
Key Laboratory of Functional and Clinical Translational Medicine, Department of Basic Medicine, Xiamen Medical College, Xiamen 361023, People's Republic of China  
Tel +86-592-2110642  
Fax +86-592-2070806  
Email cszlotus@126.com

of these QDs has been a concern, which limits their biomedical and engineering applications.

Similar to group II–VI or IV–VI QDs, group III–V QDs (such as indium phosphide, InP) for optical sensing have merits in terms of high quantum yield, strong fluorescence, and resistance to photobleaching,<sup>1,6</sup> but they show lower toxicity than the QDs in the other groups because they do not have toxic heavy metal elements.<sup>7</sup> Once the core metal is released, the optical properties are decreased, and the metal ions may be toxic to cells. To reduce the release of metal elements, a shell consisting of a layer of zinc sulfide (ZnS) is usually used to coat and passivate the metal core. In addition to protecting the core material against degradation, the ZnS shell also significantly enhances the brightness and reduces the width of the emission spectrum of the QDs.<sup>1,7</sup> The core/shell structure of the InP/ZnS QDs is being recognized as a potential alternative to that of the group II–VI or IV–VI QDs. Despite significant improvements, there is still concern about the biosafety of InP/ZnS QDs. Few studies have been conducted to evaluate their ability to induce toxicity either in vivo or in vitro. For example, in mice exposed to 25 mg/kg of polyethylene glycol (PEG) phospholipid-encapsulated InP/ZnS QDs, no significant alterations in the histology or serum hepatic function were found, but the activities of aspartate transaminase (AST) and lactate dehydrogenase (LDH) were slightly increased 3 days after treatment.<sup>8</sup> However, other research has shown that exposure to 1–5 µg/mL PEG-modified InP/ZnS QDs (PEG-InP/ZnS QDs) for 72 h significantly decreased the viability of neuroblastoma (SH-SY5Y) cells.<sup>9</sup> Recently, PEG-encapsulated InP/ZnS QDs were found to induce low levels of cytotoxicity and activation in mouse “macrophage-like” RAW264.7 cells.<sup>10</sup> Given the contradictory results among different experimental models, it is essential to investigate the potential toxicity of InP/ZnS QDs, especially with regard to immunotoxicity, both in vivo and in vitro.

Both oxidative stress and endoplasmic reticulum (ER) stress are involved in inflammation.<sup>11</sup> Oxidative stress is one of the common toxic mechanisms associated with most materials and is mainly derived from reactive oxygen species (ROS).<sup>12</sup> As an important organelle, the ER is responsible for protein synthesis, modification, and transport.<sup>13</sup> Under the stressed conditions caused by hazardous materials, unfolded or misfolded proteins will accumulate in the ER, resulting in ER stress and activation of the unfolded protein response (UPR). The UPR is sensed by three branches: (1) inositol-requiring enzyme 1 $\alpha$  (IRE1 $\alpha$ ), an endonuclease that splices X-box binding

protein-1 (XBP1) mRNA, producing an XBP1 protein that transactivates the genes maintaining ER homeostasis; (2) activating transcription factor 6 (ATF6), a transcription factor that regulates the expression of ER chaperone genes; and (3) the double-stranded RNA-activated protein kinase (PKR)-like endoplasmic reticulum kinase (PERK), which suppresses the translation of most mRNAs, except ATF4, by phosphorylating eukaryotic protein synthesis initiation factor 2 $\alpha$  (eIF2 $\alpha$ ). As a transcription factor, ATF4 regulates many genes involved in ER homeostasis, cell survival, autophagy, and inflammation to safeguard cell homeostasis.<sup>14</sup> Moreover, oxidative stress and ER stress interact with each other such that ROS can induce ER stress.<sup>15</sup> Recently, a few nanoparticles (NPs) have been reported to trigger ER stress and oxidative stress, including zinc oxide (ZnO) NPs,<sup>16</sup> silica NPs,<sup>17</sup> superparamagnetic iron oxide NPs,<sup>18,19</sup> and CdTe-QDs.<sup>20</sup>

In the present study, mice and their bone marrow-derived macrophages (BMMs) were exposed to PEG-InP/ZnS QDs. We found that PEG-InP/ZnS QDs could increase the number of neutrophils in mice and induce inflammatory responses, oxidative stress and ER stress in the BMMs. Furthermore, the inhibition of the oxidative stress or the ER stress could attenuate the inflammatory response caused by the PEG-InP/ZnS QDs. Of the UPR-sensing pathways described above, the PERK-ATF4 branch may be the main pathway by which the inflammation induced by macrophages is regulated. The findings from this research are expected to be helpful for understanding the biocompatibility of InP/ZnS QDs and for promoting their safe application in engineering nanomaterials or nanomedicines.

## Materials and Methods

### Characterization of the InP/ZnS QDs

Carboxyl PEG-InP/ZnS QDs were purchased from Xingzi New Material Technology Development Co. Ltd. (Shanghai, China). The UV–VIS absorption and photoluminescence spectra of the PEG-InP/ZnS QDs were assessed using a multiscan spectrum microplate reader (Tecan, Männedorf, Switzerland). QD size was measured with a 200 KV transmission electron microscope (TEM, JEOL, Tokyo, Japan). The zeta potential was examined with a Zetasizer (Nano ZS90, Malvern, Worcestershire, UK).

### Reagents

*Escherichia coli* lipopolysaccharides (LPS), N-acetylcysteine (NAC), diphenylene iodonium (DPI), mito-TEMPO,

tauroursodeoxycholic acid (TUDCA) and 4-phenylbutyric acid (4-PBA) were obtained from Sigma-Aldrich (St. Louis, MO, USA). Macrophage colony-stimulating factor (M-CSF) was obtained from PeproTech (Rocky Hill, NJ, USA). Dulbecco's modified Eagle's medium (DMEM) was purchased from HyClone (Logan, UT, USA). Fetal bovine serum (FBS) was provided by Gibco (Waltham, MA, USA).

## Mice

Eight-week-old female C57BL/6 mice weighing 17–19 g were purchased from SLAC Laboratory Animal Co., Ltd. (Shanghai, China) and randomly housed in cages (five mice per cage). They were maintained in specific pathogen-free (SPF) facilities under a constant temperature of  $22 \pm 3$  °C and relative humidity of  $40 \pm 10\%$ , with free access to water and food under a 12 h light/dark cycle at the Xiamen medical college. All animal studies were performed in compliance with the guidelines of the Institutional Animal Care and Use Committee under the approval of the Administrative Committee of Laboratory Animals of Xiamen Medical College (Approval number 20180301014).

## Animal Experiments

The mice were randomly divided into two groups with six mice in each group. The mice were injected intraperitoneally with 20 mg/kg PEG-InP/ZnS QDs suspended in 200  $\mu$ L phosphate buffered saline (PBS); control mice received only PBS. Six hours after the injection, the mice were sacrificed, blood samples were harvested, and a routine examination was performed on the whole blood with a ProCyt Dx hematology analyzer (IDEXX Laboratories, Inc., Westbrook, ME, USA). For the interleukin-6 (IL-6) measurements, 600  $\mu$ L of PBS with 1% (v/v) FBS was used, and IL-6 level in the supernatant of the peritoneal lavage fluid (PLF) was determined. Then, peritoneal cells were obtained with 10 mL PBS with 1% (v/v) FBS, centrifuged and examined with a ProCyt Dx hematology analyzer.

## Bone Marrow-Derived Macrophage Preparation and Culture

The mouse BMMs were prepared as follows: bone marrow cells were flushed from the femurs and tibias of the mice and depleted of red blood cells using ammonium chloride. The cells were seeded at  $1.5 \times 10^6$  cells per well in 24-well plates with DMEM containing 10% FBS and supplemented with 20 ng/mL murine M-CSF and incubated at 37 °C

in a humidified atmosphere containing 5% CO<sub>2</sub>. Non-adherent cells were carefully removed, and fresh medium was added every other day. On the 6th day, the cells were identified using microscopy as BMMs (Nikon, Tokyo, Japan) and were then collected for further experiments.

## BMM Treatments

The BMMs were stimulated with PEG-InP/ZnS QDs (40  $\mu$ g/mL) for 24 h. For pharmacological assessments, TUDCA (200  $\mu$ M), 4-PBA (2.5 mM), mito-TEMPO (50  $\mu$ M), NAC (10 mM) or DPI (12.5 mM) were added to the media 15 min before the PEG-InP/ZnS QD treatment.

## MTS Assay

Cell viability was determined with the MTS assay kit (Promega, WI, USA) according to the manufacturer's instructions. Briefly, approximately  $2 \times 10^5$  BMMs were seeded per well in 96-well plates and treated with 2.5, 5, 10, 20, 40, or 80  $\mu$ g/mL PEG-InP/ZnS QDs for 24 h. MTS (20  $\mu$ L/well) was added to the plates before they were incubated for another 2–3 h. The optic density (OD) of the formazan products was measured at 490 nm with a multifunctional microplate system (Multiscan, Thermo, CO, USA).

## mRNA Extraction and Quantitative Real-Time PCR

Total RNA was extracted from the BMMs with TRIzol (Invitrogen) according to the manufacturer's instructions. Oligo(dT) priming and Moloney murine leukemia virus reverse transcriptase (Invitrogen) were used for the reverse transcription of the purified RNA. All of the gene transcripts were quantified by real-time PCR with 2 $\times$ SYBR Green qPCR Master Mix and a QuantStudio 5 Real-Time PCR system (Applied Biosystems, Foster City, CA). The relative fold induction was calculated by the comparative CT ( $2^{-\Delta\Delta CT}$ ) method. The sequences of primers for real-time PCR analysis were as follows: *Il-6*, forward, 5' CCC ACC AAG AAC GAT AGT CAA T 3', and reverse, 5' CAT TTC CAC GAT TTC CCA GAG 3'; *glyceraldehyde-3-phosphate dehydrogenase (Gapdh)*, forward, 5' TTG ATG GCA ACA ATC TCC AC 3', and reverse, 5' CGT CCC GTA GAC AAA ATG GT 3'; *nitric oxide synthase 2 (Nos2)*, forward, 5' GGA GCG AGT TGT GGA TTG TC 3', and reverse, 5' GTG AGG GCT TGG CTG AGT G 3'; *Hspa5*, forward, 5' AAC CAA CTC ACG TCC AAC CC 3', and reverse, 5' TCT TTC CCA AAT ACG CCT CAG

3'; *Perk*, forward, 5' GGA GAC AGT GTT TGG CTT AGG G 3', and reverse, 5' GGC ATC CAG TGC AGC GAT T 3'; *Irela*, forward, 5' CCA GGA TGT AAG TGA CCG AAT AG 3', and reverse, 5' GGA AGC GGG AAG TGA AGT AG 3'; *Atf6*, forward, 5' CAG ACA CTA CCA GCC CTT ATG C 3', and reverse, 5' TTG TAG AAC AGG TTT AGT CAC GG 3'; *Atf4*, forward, 5' GCC AAG CAC TTG AAA CCT CA 3', and reverse, 5' CTC CAA CAT CCA ATC TGT CCC 3'; and *C/EBP-homologous protein (Chop)*, forward, 5' CCT GCC TTT CAC CTT GGA G 3', and reverse, 5' AGC GAG GGC TTT GGG ATG T 3'.

## Enzyme-Linked Immunosorbent Assay (ELISA)

Mouse IL-1 $\beta$ , IL-6, and TNF- $\alpha$  ELISA kits were purchased from R&D Company (Minneapolis, MN, USA). These cytokines were measured in culture supernatants with the corresponding ELISA kits according to the manufacturer's instructions.

## Intracellular and Mitochondrial ROS Assay

The production of intracellular ROS and mitochondrial ROS (mtROS) was detected using a reactive oxygen species assay kit (Beyotime, Shanghai, China) and MitoSOX<sup>TM</sup> Red Mitochondrial Superoxide Indicator (Molecular Probes, Waltham, MA, USA) according to the manufacturers' protocols. After treatment with PEG-InP/ZnS QDs for 24 h, the cells were incubated with 10  $\mu$ M 2',7'-dichlorodihydrofluorescein diacetate (DCFH-DA) or 5  $\mu$ M MitoSOX<sup>TM</sup> Red in serum-free

medium at 37  $^{\circ}$ C for 20 min in the dark. After the cells were washed 3 times, the fluorescence intensity was analyzed using flow cytometry (FACS Calibur, BD, USA).

## Statistical Analysis

The results from the statistical analysis are presented as the mean  $\pm$  standard error (SE). Statistical comparisons between different treatments were determined by using the unpaired Student's *t*-test and one-way analysis of variance (ANOVA) (Prism 7 software, version 7.0a, GraphPad, San Diego, CA, USA). For all tests, the value of  $P < 0.05$  or  $P < 0.01$  was considered to be statistically significant or highly significant, respectively.

## Results

### Characterization of the InP/ZnS QDs

The shape and size of the InP/ZnS QDs were determined using TEM images, and the average size was  $12.52 \pm 1.70$  nm (Figure 1A). The zeta potential was  $-11.2 \pm 1.1$  mV. The UV-VIS absorption spectra of the InP/ZnS QDs presented a peak at 562 nm, emitting yellow (Figure 1B). The photoluminescence spectra showed an emission peak at 618 nm, fluorescing red under UV stimulation (Figure 1C).

### InP/ZnS QD Exposure Caused Acute Phase Inflammation in the Mice

To investigate the effect of InP/ZnS QD exposure on the infiltration of neutrophils, we examined the percentage of neutrophils in the PLF and blood. As shown in Figure 2, the InP/ZnS QD treatment did not significantly alter the

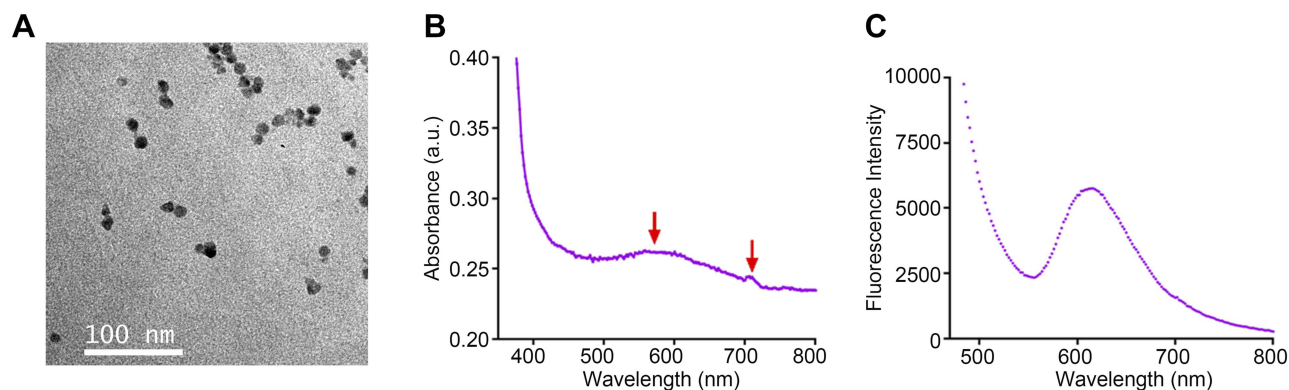


**Figure 1** Characterization of the InP/ZnS QDs. (A) TEM image of InP/ZnS QDs, with a 100 nm scale bar, displaying an average size of  $12.52 \pm 1.70$  nm. (B) The UV-VIS absorption spectrum with a peak at 562 nm (the left red arrow) showing as yellow color, while the right one at over 700 nm is out of visible light range. (C) The photoluminescence spectrum of InP/ZnS QDs with an emission peak at 618 nm.

**Abbreviations:** QDs, quantum dots; TEM, transmission electron microscopy.

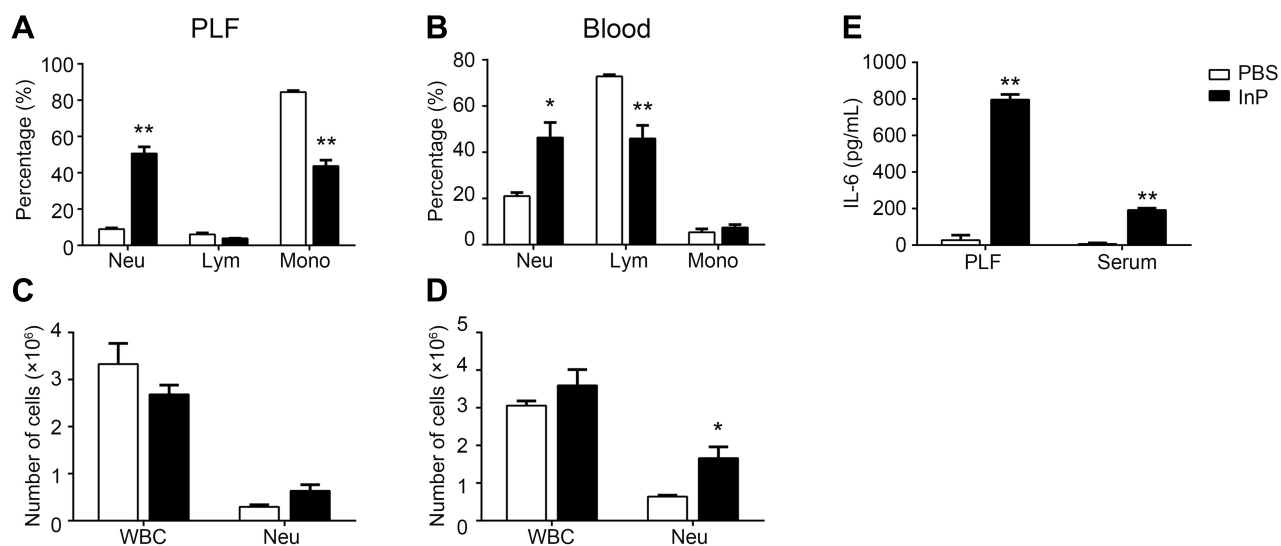


**Figure 2** InP/ZnS QD exposure induces acute phase inflammation in mice. After mice were treated with 20 mg/kg InP/ZnS QDs, the percentage of neutrophils, lymphocytes and monocytes was determined in the PLF (A) and in the blood (B), as was the number of WBCs and neutrophils in the PLF (C) and in the blood (D), as measured with a ProCyte Dx hematology analyzer. The IL-6 levels (E) in the PLF and serum were measured by ELISA. Results are representative of three independent experiments. Data are expressed as the mean  $\pm$  SE,  $n = 6$ , \* $P < 0.05$ , \*\* $P < 0.01$ , compared to the PBS controls.

**Abbreviations:** QDs, quantum dots; PLF, peritoneal lavage fluids; Neu, neutrophils; Lym, lymphocytes; Mono, monocytes; WBC, white blood cell; IL-6, interleukin-6.

total number of white blood cells (WBC, Figure 2C and D), while the percentage of neutrophils increased from  $8.97 \pm 1.17\%$  to  $50.63 \pm 7.37\%$  in the PLF (Figure 2A) and from  $21.03 \pm 2.68\%$  to  $46.37 \pm 11.30\%$  in the blood (Figure 2B), respectively, after InP/ZnS QD treatment. The number of neutrophils increased from  $(0.30 \pm 0.07) \times 10^6$  to  $(0.63 \pm 0.23) \times 10^6$  in the PLF (Figure 2C) and  $(0.64 \pm 0.06) \times 10^6$  to  $(1.66 \pm 0.52) \times 10^6$  in the blood (Figure 2D). With the increase of neutrophils, the percentages of lymphocytes and monocytes decreased in the PLF, but only the percentage of lymphocytes were significantly reduced in blood. The results indicate that InP/ZnS QD peritoneal injection can cause the infiltration of neutrophils, resulting in acute phase inflammation in mice.

### InP/ZnS QD Exposure Elevated the Amount of IL-6 Released in the Mice

To further validate that the acute phase inflammation was caused by InP/ZnS QD exposure, we measured the levels of several inflammatory factors, namely, IL-1 $\beta$ , IL-6, and TNF- $\alpha$  in the PLF and the serum from mice treated with InP/ZnS QDs. As depicted in Figure 2E, the level of IL-6 was significantly increased both in the PLF and serum, at  $29.28 \pm 1.79$ -fold and  $31.74 \pm 2.95$ -fold over the control, respectively. In contrast, neither IL-1 $\beta$  nor TNF- $\alpha$  was detected in either the PLF or the serum.

### InP/ZnS QD Exposure Increased the Expression of Inflammation-Related Genes and Enhanced IL-6 Release in the BMMs

To explore the mechanism by which InP/ZnS QDs induce acute phase inflammation, BMMs were used. First, we measured the cell viability of the BMMs after they were exposed to InP/ZnS QDs for 24 h. As shown in Figure 3, between 2.5 and 80  $\mu\text{g/mL}$  InP/ZnS QDs did not significantly alter the cell viability. Next, we examined the levels of gene expression and released pro-inflammatory cytokines in the BMMs treated with the InP/ZnS QDs. As shown in Figure 4A, InP/ZnS QD (40  $\mu\text{g/mL}$ ) treatment significantly upregulated the expression of *Il-6* and *Nos2*, by  $218.09 \pm 23.00$ -fold and  $115.05 \pm 4.22$ -fold, respectively, over the levels expressed by the control. Moreover, consistent with the findings in vivo, the level of IL-6 was also increased in the BMMs after InP/ZnS QD exposure in a concentration-dependent manner (Figure 4B).

### InP/ZnS QD-Induced Acute Phase Inflammation Could Be Alleviated by ER Stress Inhibitors

Previous studies have indicated that acute phase inflammation might be regulated by ER stress.<sup>15,19</sup> Therefore, we quantified the expression levels of the following ER stress-related genes *Hspa5* (encoding GRP78), *Perk*,

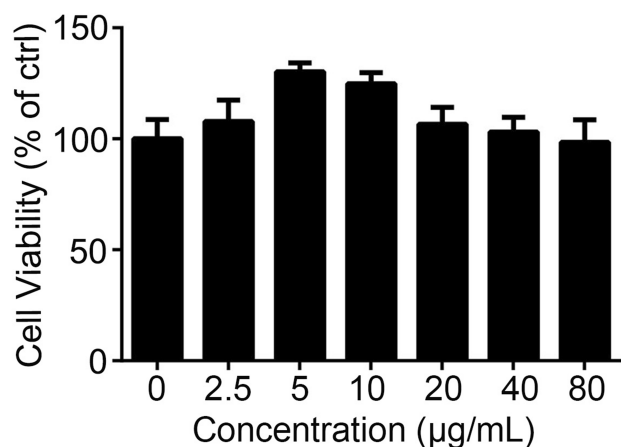


**Figure 3** Effects of InP/ZnS QDs on the cell viability of the BMMs. After BMMs were incubated with 2.5, 5, 10, 20, 40, and 80 µg/mL InP/ZnS QDs for 24 h. Cell viability was detected using an MTS assay. Results are representative of three independent experiments.

**Abbreviations:** QDs, quantum dots; BMMs, bone marrow-derived macrophages.

*Irela*, *Atf6*, *Atf4*, and *Chop* in BMMs after InP/ZnS QD (40 µg/mL) treatment. As shown in Figure 5A, the expression levels of *Perk*, *Atf4*, and *Chop* were significantly upregulated, by  $3.25 \pm 0.05$ -fold,  $1.56 \pm 0.08$ -fold, and  $1.48 \pm 0.01$ -fold over the levels expressed by the control, respectively. However, BMM exposure to InP/ZnS QDs did not increase the expression levels of *Hspa5*, *Irela*, or *Atf6*. Furthermore, pretreatment with TUDCA or 4-PBA, two kinds of ER stress inhibitors, significantly decreased the IL-6 level expression, from  $1267.57 \pm 8.33$  pg/mL to  $508.96 \pm 8.68$  pg/mL and  $139.53 \pm 4.47$  pg/mL,

respectively (Figure 5B). These data suggested that acute phase inflammation caused by InP/ZnS QDs might be mediated by ER stress in macrophages.

### InP/ZnS QD-Induced Acute Phase Inflammation Could Be Attenuated by ROS Scavengers

ROS were also reported to be involved in acute phase inflammation.<sup>15</sup> To investigate whether ROS contributed to the InP/ZnS QD-induced acute phase inflammation in macrophages, we measured the intracellular ROS and the mtROS. As illustrated in Figure 6A and B, 40 µg/mL InP/ZnS QD exposure increased the intracellular ROS in the BMMs from  $11.85 \pm 1.03\%$  to  $15.40 \pm 0.13\%$  and the mtROS from  $20.60 \pm 1.34\%$  to  $44.30 \pm 0.94\%$ . Then, we discovered that both the intracellular ROS scavengers, NAC and DPI, and the mtROS scavenger, mito-TEMPO, could significantly reduce the amount of IL-6 released from the BMMs as induced by the InP/ZnS QDs (Figure 6C). These results showed that InP/ZnS QDs could trigger oxidative stress, which contributed to IL-6-related acute phase inflammation in macrophages.

### Discussion

In the past decade, several kinds of non-Cd/Pb QDs have been developed to reduce the health and environmental risks of toxic metal released from Cd/Pb-containing QDs. InP/ZnS QDs are one of the safer alternatives for

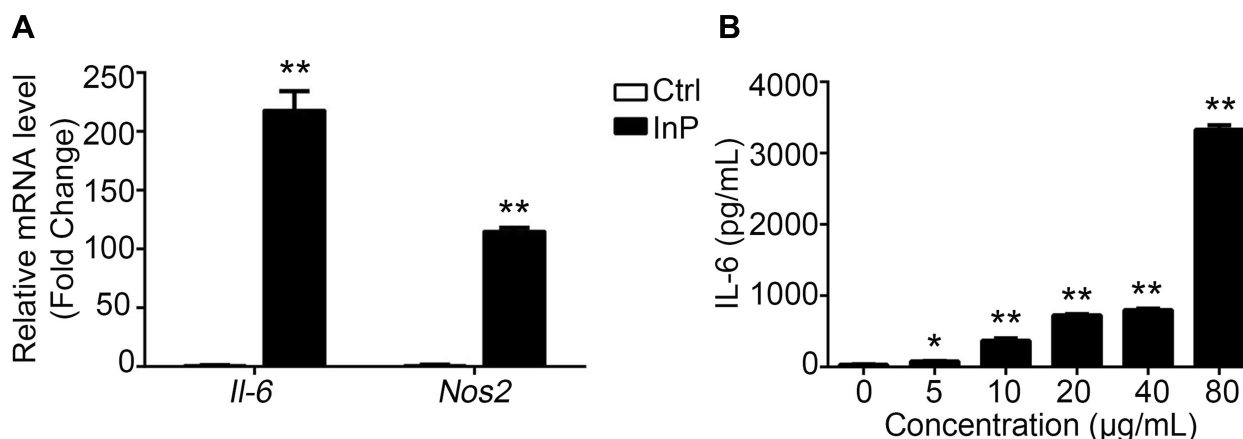


**Figure 4** InP/ZnS QD exposure triggers acute phase inflammation in macrophages. (A) After BMMs were incubated with 40 µg/mL InP/ZnS QDs for 24 h, the expression levels of *Il-6* and *Nos2* mRNA were detected with qRT-PCR. *Gapdh* was used as the reference gene. (B) After the BMMs were incubated with 5, 10, 20, 40 and 80 µg/mL InP/ZnS QDs for 24 h, IL-6 secretion was measured by ELISA. Results are representative of three independent experiments. \* $P < 0.05$  and \*\* $P < 0.01$ , compared to the untreated controls.

**Abbreviations:** QDs, quantum dots; BMMs, bone marrow-derived macrophages; IL-6, interleukin-6; Nos2, nitric oxide synthase 2; *Gapdh*, glyceraldehyde-3-phosphate dehydrogenase; ELISA, enzyme-linked immunosorbent assay.

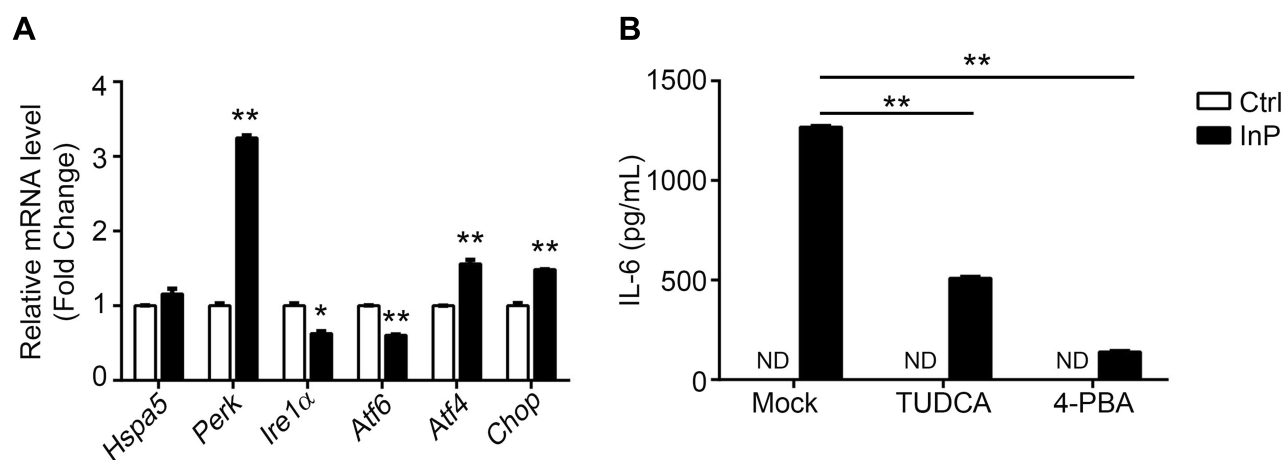


**Figure 5** ER stress is involved in IL-6 release caused by InP/ZnS QDs in macrophages. **(A)** After BMMs were incubated with 40  $\mu\text{g/mL}$  InP/ZnS QDs for 24 h, the mRNA expression of genes related to ER stress was detected with qRT-PCR. *Gapdh* was used as the reference gene. **(B)** After blocking ER stress with TUDCA (200  $\mu\text{M}$ ) or 4-PBA (2.5 mM) for 15 min, BMMs were treated with InP/ZnS QDs for 24 h. IL-6 release was measured by ELISA. Results are representative of three independent experiments. \* $P < 0.05$ , \*\* $P < 0.01$ , compared to the controls.

**Abbreviations:** ER, endoplasmic reticulum; IL-6, interleukin-6; QDs, quantum dots; BMMs, bone marrow-derived macrophages; *Gapdh*, glyceraldehyde-3-phosphate dehydrogenase; TUDCA, tauroursodeoxycholic acid; 4-PBA, 4-phenylbutyric acid; ELISA, enzyme-linked immunosorbent assay; ND, not detected.

engineering and biomedical applications. However, there are limited safety assessment studies on InP/ZnS QDs, particularly with regard to immunotoxicity and its mechanism. In our study, we focused on the acute immune response induced by InP/ZnS QDs both in vivo and in vitro. We found that InP/ZnS QD exposure increased the percentage of neutrophils and IL-6 levels in mouse PLF and blood, which led to acute phase inflammation in the mice. Consistently, IL-6 levels were also elevated in macrophages exposed to InP/ZnS QDs. Significantly, our study demonstrated that oxidative stress and ER stress through the PERK-ATF4 pathway contributes to the inflammatory response caused by InP/ZnS QDs in macrophages.

Generally, inflammation is induced to protect the body from potentially hazardous environmental factors, such as microbe infection and pollutant exposure, through cytokine release and immune cell recruitment. The release of cytokines often signal danger to recruit immune cells to injured cells or tissues.<sup>15</sup> The migration of leukocytes from blood to damaged cells or tissues is called acute phase inflammation.<sup>21</sup> The innate immune response to hazardous factors is primarily mediated by neutrophils.<sup>22</sup> In this study, we found that neutrophils infiltrated into the peritoneal cavity, which was the primary site of the injury that developed in the 6 h after the mice were injected intraperitoneally with PEG-InP/ZnS QDs. On the other hand, lymphocytes and monocytes, which are thought to be involved in the late phase of inflammation,<sup>23</sup> were decreased in the PLF.

Peripheral blood monocytes are reported to be recruited alongside neutrophils in acute inflammation.<sup>24</sup> In line with these reports, our results showed that the percentage of monocytes were slightly increased while the percentage of lymphocytes were reduced in the blood.

In this study, we found that a 24 h treatment with 2.5 to 80  $\mu\text{g/mL}$  InP/ZnS QDs did not significantly alter the cell viability of the BMMs. In detail, the cell viability was slightly enhanced with low doses of InP/ZnS QDs, which might be reflect an effect called “hormesis”.<sup>25</sup> The concept of hormesis, as an adaptive response of biological systems to cope with environmental challenges, has raised considerable interest with respect to nanotoxicology in view of the rapid pace of the production and application of increasingly innovative nanomaterials and the expected increased likelihood of environmental and human exposure to low-dose concentrations.<sup>25,26</sup> For example, Choi et al reported that a low dose of silver NPs (AgNPs) could induce hormesis in astrogloma cells<sup>27</sup> and lung epithelial cells.<sup>28</sup> We hypothesize that the increase in the cell viability of macrophages induced by low concentrations of QDs might be the result of hormesis.

Oxidative stress contributes to the toxicity induced by chemicals by producing intracellular ROS. ROS are reactive species harboring forms of oxygen, such as  $\text{O}_2^-$ ,  $\text{H}_2\text{O}_2$ , and OH. Previous studies have shown that many NPs can induce excessive ROS that cause toxicity both in vivo and in vitro. For example, He et al reported that iron oxide NPs disrupted the electron transport chain and

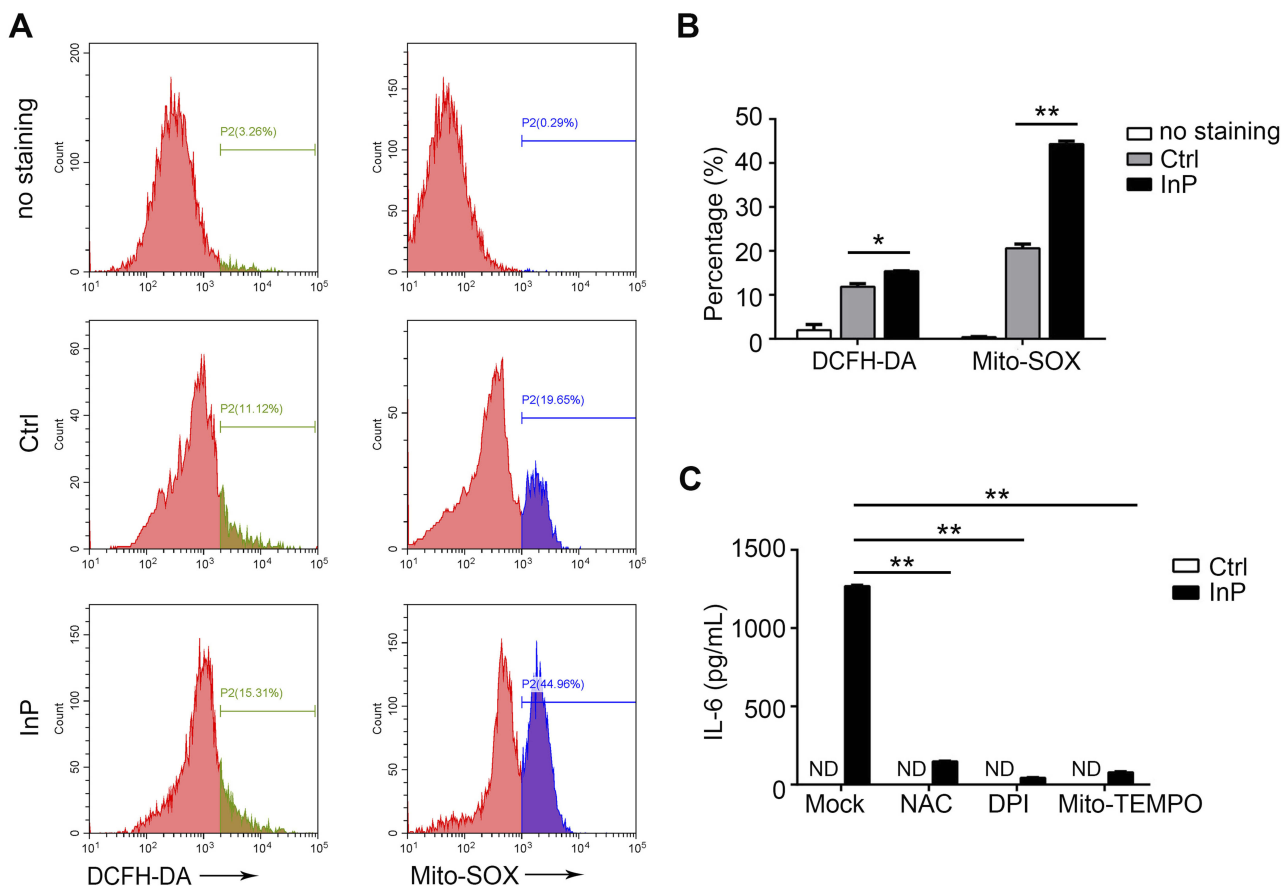


**Figure 6** IL-6 upregulation caused by InP/ZnS QD exposure can be alleviated by ROS scavengers in macrophages. **(A, B)** After treatment with InP/ZnS QDs for 24 h, the BMMs were stained with DCFH-DA or MitoSOX. The intracellular ROS and the mtROS were measured with flow cytometry **(A)**. The levels of intracellular ROS and mtROS are presented as bar graphs **(B)**. **(C)** After scavenging ROS with NAC (10 mM), DPI (12.5 mM), or mito-TEMPO (50  $\mu$ M) for 15 min, the BMMs were treated with InP/ZnS QDs for 24 h. IL-6 release was measured with ELISA. The results are representative of three independent experiments. \* $P < 0.05$  and \*\* $P < 0.01$ , compared to the controls. **Abbreviations:** IL-6, interleukin-6; QDs, quantum dots; ROS, reactive oxygen species; BMMs, bone marrow-derived macrophages; DCFH-DA, 2',7'-dichlorodihydrofluorescein diacetate; mtROS, mitochondrial ROS; NAC, N-acetylcysteine; DPI, diphenylene iodonium; ELISA, enzyme-linked immunosorbent assay; ND, not detected.

generated mtROS, resulting in apoptosis of hepatic cancer cells.<sup>18</sup> The cytotoxicity of CdSe/ZnS QDs was reported to correlate with the level of ROS and mtROS in human foreskin fibroblast cell lines.<sup>29</sup> Recently, Wang et al reported that InP/ZnS QD exposure increased the intracellular ROS level in human lung cancer HCC-15 cells and alveolar type II epithelial RLE-6TN cells.<sup>30</sup> In our study, we also found that InP/ZnS-QDs elevated the levels of intracellular ROS and mtROS in macrophages. Furthermore, depletion of intracellular ROS or mtROS with its corresponding scavengers reduced the level of IL-6 triggered by InP/ZnS-QDs. These results demonstrate that the InP/ZnS-QD-induced acute phase inflammation is under the regulation of intracellular ROS and mtROS in macrophages.

The ER is an organelle responsible for protein synthesis and folding.<sup>13</sup> ER stress is involved in the inflammatory

response by promoting the generation of cytokines, such as IL-6.<sup>19</sup> For example, previous studies showed that LPS triggered macrophages to generate mature IL-1 $\beta$ , and ATF4 played an essential role in IL-1 $\beta$  generation.<sup>31,32</sup> Recently, the ER stress-related PERK-ATF4 pathway was demonstrated to regulate IL-6 expression and release in hepatic cells treated with iron oxide NPs.<sup>19</sup> In this study, the PERK-ATF4 pathway was also activated by InP/ZnS-QD exposure of macrophages. We further found that blocking ER stress with inhibitors decreased the release of IL-6. These studies indicate that the ER stress-related PERK-ATF4 pathway also contributes to the acute phase inflammation caused by InP/ZnS-QDs.

## Conclusions

In summary, our study demonstrated that InP/ZnS QD exposure could promote the migration and infiltration of neutrophils and the release of IL-6 in a mouse model.

Consistently, InP/ZnS QDs activated mouse macrophages and triggered the production of IL-6. InP/ZnS QD exposure also caused oxidative stress and ER stress in the macrophages. Moreover, blocking the oxidative stress or the ER stress could alleviate the acute phase inflammation caused by the InP/ZnS QDs. Our work illuminates the biocompatibility of the InP/ZnS QDs and describes the mechanism by which they induce immunotoxicity, information that is expected to be beneficial for the safe application of InP/ZnS QDs in biomedical and engineering fields.

## Abbreviations

QDs, quantum dots; BMMs, bone marrow-derived macrophages; IL-6, interleukin-6; InP, indium phosphide; ZnS, zinc sulfide; ER, endoplasmic reticulum; AST, aspartate transaminase; LDH, lactate dehydrogenase; PEG, polyethylene glycol; ROS, reactive oxygen species; UPR, unfolded protein response; IRE1 $\alpha$ , inositol-requiring enzyme 1 $\alpha$ ; XBP1, X-box binding protein-1; ATF6, activating transcription factor 6; PERK, protein kinase (PKR)-like endoplasmic reticulum kinase; eIF2 $\alpha$ , eukaryotic protein synthesis initiation factor 2 $\alpha$ ; NPs, nanoparticles; ZnO, zinc oxide; TEM, transmission electron microscopy; PLF, peritoneal lavage fluid; Gapdh, glyceraldehyde-3-phosphate dehydrogenase; Nos2, nitric oxide synthase 2; Chop, C/EBP-homologous protein; TUDCA, tauroursodeoxycholic acid; 4-PBA, 4-phenylbutyric acid; NAC, N-acetylcysteine; DPI, diphenylene iodonium; LPS, lipopolysaccharides; M-CSF, macrophage-colony stimulating factor; DMEM, Dulbecco's modified Eagle's medium; FBS, fetal bovine serum; PBS, phosphate buffered saline; SPF, specific-pathogen-free; ELISA, enzyme-linked immunosorbent assay; mtROS, mitochondrial ROS; DCFH-DA, 2',7'-dichlorodihydrofluorescein diacetate; WBC, white blood cell; ND, not detected.

## Ethics Approval and Consent to Participate

All animal studies were performed in compliance with the guidelines of the Institutional Animal Care and Use Committee under the approval of the Administrative Committee of Laboratory Animals of Xiamen Medical College (Approval number 20180301014).

## Acknowledgements

This work was supported by the Training Program of Outstanding Young Scientific Researcher of Fujian

College, the Key Project of Natural Science Foundation for Young Scholars of Fujian College (No. JZ160496), the Education Scientific Research Project of Young Teachers of Fujian Province (No. JT180650), and the Innovation and Entrepreneurship Training Program for Undergraduates of Fujian Province (No. 201812631013).

## Disclosure

The authors report no conflicts of interest in this work.

## References

- Tamang S, Beaune G, Texier I, Reiss P. Aqueous phase transfer of InP/ZnS nanocrystals conserving fluorescence and high colloidal stability. *ACS Nano*. 2011;5(12):9392–9402. doi:10.1021/nn203598c
- Gao J, Chen K, Luong R, et al. A novel clinically translatable fluorescent nanoparticle for targeted molecular imaging of tumors in living subjects. *Nano Lett*. 2012;12(1):281–286. doi:10.1021/nl203526f
- Kumar BG, Sadeghi S, Melikov R, et al. Structural control of InP/ZnS core/shell quantum dots enables high-quality white LEDs. *Nanotechnology*. 2018;29(34):345605. doi:10.1088/1361-6528/aac8c9
- Zarco-Fernandez S, Coto-Garcia AM, Munoz-Olivas R, Sanz-Landaluze J, Rainieri S, Camara C. Bioconcentration of ionic cadmium and cadmium selenide quantum dots in zebrafish larvae. *Chemosphere*. 2016;148:328–335. doi:10.1016/j.chemosphere.2015.12.077
- Wieczinski PN, Metz KM, King Heiden TC, et al. Toxicity of oxidatively degraded quantum dots to developing zebrafish (*Danio rerio*). *Environ Sci Technol*. 2013;47(16):9132–9139. doi:10.1021/es304987r
- Panzer R, Guhrenz C, Haubold D, et al. Versatile Tri(pyrazolyl) phosphanes as Phosphorus Precursors for the synthesis of highly emitting InP/ZnS Quantum dots. *Angew Chem Int Ed Engl*. 2017;56(46):14737–14742. doi:10.1002/anie.201705650
- Brunetti V, Chibli H, Fiammengo R, et al. InP/ZnS as a safer alternative to CdSe/ZnS core/shell quantum dots: *in vitro* and *in vivo* toxicity assessment. *Nanoscale*. 2013;5(1):307–317. doi:10.1039/C2NR33024E
- Lin G, Ouyang Q, Hu R, et al. *In vivo* toxicity assessment of non-cadmium quantum dots in BALB/c mice. *Nanomedicine*. 2015;11(2):341–350. doi:10.1016/j.nano.2014.10.002
- Liu J, Hu R, Liu J, et al. Cytotoxicity assessment of functionalized CdSe, CdTe and InP quantum dots in two human cancer cell models. *Mater Sci Eng C Mater Biol Appl*. 2015;57:222–231. doi:10.1016/j.msec.2015.07.044
- Ayupova D, Dobhal G, Laufersky G, Nann T, Goreham RV. An *in vitro* investigation of cytotoxic effects of InP/ZnS quantum dots with different surface chemistries. *Nanomaterials (Basel)*. 2019;9(2):E135. doi:10.3390/nano9020135
- Cao SS, Luo KL, Shi L. Endoplasmic reticulum stress interacts with inflammation in human diseases. *J Cell Physiol*. 2016;231(2):288–294. doi:10.1002/jcp.v231.2
- Sarkar A, Ghosh M, Sil PC. Nanotoxicity: oxidative stress mediated toxicity of metal and metal oxide nanoparticles. *J Nanosci Nanotechnol*. 2014;14(1):730–743. doi:10.1166/jnn.2014.8752
- Krebs J, Agellon LB, Michalak M. Ca<sup>2+</sup> homeostasis and endoplasmic reticulum (ER) stress: an integrated view of calcium signaling. *Biochem Biophys Res Commun*. 2015;460(1):114–121. doi:10.1016/j.bbrc.2015.02.004
- Wang M, Kaufman RJ. Protein misfolding in the endoplasmic reticulum as a conduit to human disease. *Nature*. 2016;529(7586):326–335. doi:10.1038/nature17041

15. Dandekar A, Mendez R, Zhang K. Cross talk between ER stress, oxidative stress, and inflammation in health and disease. *Methods Mol Biol.* 2015;1292:205–214.
16. Chen R, Huo L, Shi X, et al. Endoplasmic reticulum stress induced by zinc oxide nanoparticles is an earlier biomarker for nanotoxicological evaluation. *ACS Nano.* 2014;8(3):2562–2574. doi:10.1021/nm406184r
17. Wang J, Li Y, Duan J, et al. Silica nanoparticles induce autophagosome accumulation via activation of the EIF2AK3 and ATF6 UPR pathways in hepatocytes. *Autophagy.* 2018;14(7):1185–1200. doi:10.1080/15548627.2018.1458174
18. He C, Jiang S, Jin H, et al. Mitochondrial electron transport chain identified as a novel molecular target of SPIO nanoparticles mediated cancer-specific cytotoxicity. *Biomaterials.* 2016;83:102–114. doi:10.1016/j.biomaterials.2016.01.010
19. He C, Jiang S, Yao H, et al. Endoplasmic reticulum stress mediates inflammatory response triggered by ultra-small superparamagnetic iron oxide nanoparticles in hepatocytes. *Nanotoxicology.* 2018;12(10):1198–1214. doi:10.1080/17435390.2018.1530388
20. Jiang S, Lin Y, Yao H, et al. The role of unfolded protein response and ER-phagy in quantum dots-induced nephrotoxicity: an *in vitro* and *in vivo* study. *Arch Toxicol.* 2018;92(4):1421–1434. doi:10.1007/s00204-018-2169-0
21. Rock KL, Kono H. The inflammatory response to cell death. *Annu Rev Pathol.* 2008;3:99–126. doi:10.1146/annurev.pathmechdis.3.121806.151456
22. Nathan C. Neutrophils and immunity: challenges and opportunities. *Nat Rev Immunol.* 2006;6(3):173–182. doi:10.1038/nri1785
23. Zuelli FM, Carnio EC, Saia RS. Cholecystokinin protects rats against sepsis induced by *Staphylococcus aureus*. *Med Microbiol Immunol.* 2014;203(3):165–176. doi:10.1007/s00430-014-0328-3
24. Dhaliwal K, Scholefield E, Ferenbach D, et al. Monocytes control second-phase neutrophil emigration in established lipopolysaccharide-induced murine lung injury. *Am J Respir Crit Care Med.* 2012;186(6):514–524. doi:10.1164/rccm.201112-2132OC
25. Iavicoli I, Leso V, Fontana L, Calabrese EJ. Nanoparticle exposure and hormetic dose-responses: an update. *Int J Mol Sci.* 2018;19:3. doi:10.3390/ijms19030805
26. Fisher P. Homeopathy, hormesis, nanoparticles and nanostructures. *Homeopathy.* 2015;104(2):67–68. doi:10.1016/j.homp.2015.03.002
27. Choi JH, Min WK, Gopal J, et al. Silver nanoparticle-induced hormesis of astroglia cells: a Mu-2-related death-inducing protein-orchestrated modus operandi. *Int J Biol Macromol.* 2018;117:1147–1156. doi:10.1016/j.ijbiomac.2018.05.234
28. Sthijns MM, Thongkam W, Albrecht C, et al. Silver nanoparticles induce hormesis in A549 human epithelial cells. *Toxicol in Vitro.* 2017;40:223–233. doi:10.1016/j.tiv.2017.01.010
29. Manshian BB, Martens TF, Kantner K, et al. The role of intracellular trafficking of CdSe/ZnS QDs on their consequent toxicity profile. *J Nanobiotech.* 2017;15(1):45.
30. Wang X, Tian J, Yong KT, et al. Immunotoxicity assessment of CdSe/ZnS quantum dots in macrophages, lymphocytes and BALB/c mice. *J Nanobiotech.* 2016;14:10. doi:10.1186/s12951-016-0162-4
31. Shenderov K, Riteau N, Yip R, et al. Cutting edge: endoplasmic reticulum stress licenses macrophages to produce mature IL-1 $\beta$  in response to TLR4 stimulation through a caspase-8- and TRIF-dependent pathway. *J Immunol.* 2014;192(5):2029–2033. doi:10.4049/jimmunol.1302549
32. Zhang C, Bai N, Chang A, et al. ATF4 is directly recruited by TLR4 signaling and positively regulates TLR4-triggered cytokine production in human monocytes. *Cell Mol Immunol.* 2013;10(1):84–94. doi:10.1038/cmi.2012.57

## International Journal of Nanomedicine

### Publish your work in this journal

The International Journal of Nanomedicine is an international, peer-reviewed journal focusing on the application of nanotechnology in diagnostics, therapeutics, and drug delivery systems throughout the biomedical field. This journal is indexed on PubMed Central, MedLine, CAS, SciSearch®, Current Contents®/Clinical Medicine,

Journal Citation Reports/Science Edition, EMBase, Scopus and the Elsevier Bibliographic databases. The manuscript management system is completely online and includes a very quick and fair peer-review system, which is all easy to use. Visit <http://www.dovepress.com/testimonials.php> to read real quotes from published authors.

Submit your manuscript here: <https://www.dovepress.com/international-journal-of-nanomedicine-journal>

Dovepress